ACS APPLIED MATERIALS & INTERFACES

Research Article

Cite This: ACS Appl. Mater. Interfaces 2017, 9, 44231−44240

www.acsami.org

A Novel Electrochemical Biosensor Based on a Double-Signal Technique for d(CAG)$_n$ Trinucleotide Repeats

Jiao Li,[‡] Yalan Liu,[‡] Xiaoqian Zhu,[‡] Gang Chang,*[,†,§] Hanping He,*[,†,‡] Xiuhua Zhang,[†,‡] and Shengfu Wang[†,‡]

[†]Hubei Collaborative Innovation Center for Advanced Organic Chemical Materials and [‡]Ministry of Education Key Laboratory for the Synthesis and Application of Organic Functional Molecules, College of Chemistry and Chemical Engineering, Hubei University, Youyi Road 368, Wuchang, Wuhan, Hubei 430062, P. R. China

[§]Ministry of Education Key Laboratory for the Green Preparation and Application of Functional Materials, School of Materials Science and Engineering, Hubei University, Youyi Road 368, Wuchang, Wuhan, Hubei 430062, China

Supporting Information

ABSTRACT: Electrochemical sensors now play an important role in analysis and detection of nucleic acids. In this work, we present a novel double-signal technique for electrochemically measuring the sequence and length of the d(CAG)$_n$ repeat. The double-signal technique used an electrochemical molecular beacon (a hairpin DNA labeled with ferrocene), which was directly modified on the surface of a gold electrode, while a reporter probe (a DNA sequence labeled with horseradish peroxidase) was hybridized to the target DNA. First a simple single-signal sensor was characterized in which d(CAG)$_n$ repeats were detected using a short reporter DNA strand labeled with horseradish peroxidase. To obtain a reliable signal that was dependent on repeat number, a double-signal biosensor was created in which the single strand capture DNA in single-signal sensor was replaced by an electrochemical molecular beacon labeled with ferrocene. When the hairpin DNA hybridized to the target−reporter DNA complex, it opened, resulting in a decreased ferrocene current. Both electrochemical biosensors exhibited high selectivity and sensitivity with low detection limits of 0.21 and 0.15 pM, respectively, for the detection of d(CAG)$_n$ repeats. The double-signal sensor was more accurate for the determination of repeat length, which was measured from the ratio of signals for HRP and ferrocene (H/F). A linear relationship was found between H/F and the number of repeats (n), H/F = 0.1398n + 9.89788, with a correlation coefficient of 0.974. Only 10 nM of target DNA was required for measurements based on the value of H/F in the double-signal technique. These results indicated that this new double-signal electrochemical sensor provided a reliable method for the analysis of CAG trinucleotide repeats.

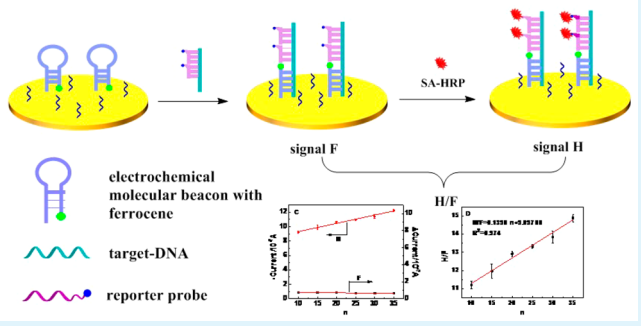

KEYWORDS: *electrochemical sensors, CAG trinucleotide repeat, double-signal technique, HRP, ferrocene*

INTRODUCTION

Trinucleotide repeats (TNRs) are common *in vivo* and can lead to neurodegenerative disease.[1,2] A number of neurodegenerative disorders were identified to have resulted from an increase in TNRs in surveys of the human genome, such as Fragile X syndrome, Friedrich's ataxia, spinocerebellar ataxias, and Kennedy's disease.[3−6] Expansions of CAG TNRs are also the mutagenic cause of 14 known neurodegenerative human disorders, including Huntington's disease and myotonic dystrophy.[6,7] Huntington's disease is a particularly challenging autosomal dominant neurodegenerative human disorder for which there is currently no cure.[8,9] The gene responsible for Huntington's disease is also essential for brain development. TNRs with different lengths can lead to different diseases. At a certain threshold length, diseases are observed, and this threshold varies by disease.[1] New DNA-level diagnostics are crucially needed for neurodegenerative diseases to confirm clinical diagnoses, especially for providing genetic screening of at-risk individuals. Current methods used to detect TNRs in the clinic mainly rely on gel electrophoresis for the detection of length of amplified DNA repeat regions or Southern blotting.

The development of DNA sensors is popular not only in chemistry but also in chemical and molecular biology. DNA biosensors are increasingly used to detect DNA sequences through DNA hybridization. Some researchers had studied expansion and biological property of CAG trinucleotide acid repeat. However, to the best of our knowledge, TNRs have rarely been measured using DNA sensors. Barros et al. demonstrated the fluorescence detection of CAG TNRs using small molecules.[10] Huang et al. proposed a differential scanning calorimetry

Received: October 10, 2017
Accepted: November 20, 2017
Published: November 20, 2017

DOI: 10.1021/acsami.7b15014
ACS Appl. Mater. Interfaces 2017, 9, 44231−44240

assay for CAG TNRs.[11] Despite the remarkable progress in DNA sensors, several drawbacks remain, including their complicated operation and expensive instrumentation.

Electrochemical DNA sensors have attracted much recent attention because of their low cost, rapid operation, small size, and low power consumption.[12−15] Common modes of electrochemical DNA sensing include chronocoulometry, differential pulse voltammetry (DPV), electrochemical impedance spectroscopy (EIS), and square-wave voltammetry (SWV). Yuan et al. described a facile and pragmatic electrochemical biosensor for the convenient detection of target DNA by integrating a homogeneous target-dependent DTITA at the biosensing interface.[16] Yang developed a cascade-amplified electrochemiluminescence biosensor for a p53 DNA sequence that combined the superior recognition capacity of NESA toward single-base mismatches and the signal amplification efficiency of HRCA.[17] Unfortunately, electrochemical DNA sensors have rarely been used to detect the sequences and repeat numbers of TNRs. Recently, we proposed a simple electrochemical biosensor with an excellent selectivity and sensitivity for the detection of CGG TNRs using a new bifunctional electrochemical probe containing a recognition portion based on NCD and an electroactive ferrocenyl group.[2,18,19] EIS (electrochemical impedance spectroscopy) sensors were also studied by recognize organic molecules modified electrode.[15] These studies have provided some approaches to detect TNRs electrochemically, which is important for the early diagnosis and treatment of neurodegenerative diseases associated with TNRs.

HRP (horseradish peroxidase) is widely used in electrochemical analysis, medical diagnostics, biological analysis, chemical manufacturing, and pollutant purification because of its excellent efficiency and substrate specificity. Peroxidase catalyzes the oxidation of electron donors in the presence of peroxide.[20] In the presence of TMB (3,3′,5,5′-tetramethylbenzidine), HRP is an enzyme that efficiently catalyzes the reduction of hydrogen peroxide, which can be measured electrochemically to quantitatively reflect the amount of DNA present.[21] We chose to use HRP as a reporter probe in this work because of its stability and excellent repeatability.

A series of strategies have been developed to improve the sensitivity and selectivity of electrochemical DNA detection. Among them, the "sandwich structure" strategy is popular.[22,23] Here we propose a new electrochemical strategy, a double-signal technique, which include the electrochemical molecular beacon with ferrocene that was directly modified on the surface of a gold electrode, and a reporter probe with HRP that was hybridized to the target DNA. Importantly, this electrochemical method allows the length of the repeat to be detected, based on multiple hybridizations of a repetitive DNA sequence with a short reporter probe. In this work, amperometric $i-t$ curves and SWV were used to measure sequence selectivity, concentration, and length of d$(CAG)_n$ TNRs. These new electrochemical biosensors exhibited excellent selectivities and sensitivities with a low limit of detection (LOD) of 0.15 pM. These biosensors have great potential as early warning and clinical diagnosis tools for neurodegenerative diseases.

EXPERIMENTAL SECTION

Reagents and Materials. HRP-conjugated streptavidin (SA-HRP) was purchased from Sangon Biotech Co., Ltd. (Shanghai, China). 6-Mercapto-1-hexanol (MCH) was obtained from J&K Chemical, Ltd. Tris(2-carboxyethyl)phosphine hydrochloride (TCEP) was obtained from Sigma-Aldrich (USA). H_2O_2 (30%) and 3,3′,5,5′-tetramethylbenzidine (TMB) were purchased from Aladdin Industrial Co. (Shanghai, China). All other reagents were of analytical grade and used without further purification. In this work, 0.1 M phosphate buffered saline (PBS, pH 5 or 7.4) was used as the supporting electrolyte. All aqueous solutions were prepared with ultrapure water (18.25 MΩ cm) from an aquapro water purification system. All synthetic DNA sequences (see the Supporting Information) were provided by Sangon Biotech Co., Ltd. (Shanghai, China).

Apparatus. Cyclic voltammetry (CV) and EIS measurements were performed with a CHI 660E electrochemical workstation (CH Instruments, Shanghai, China). A platinum wire and a saturated calomel electrode (SCE) were used as counter and reference electrodes, respectively. The gold electrodes (GE) with 2 mm diameter were used as the working electrode.

Fabrication of Electrochemical Biosensor. The GE was polished with a 0.05 μm Al_2O_3 slurry. After polishing, the electrodes were sonicated once in ethanol and twice in ultrapure water for 5 min. These electrodes were then electrochemically cleaned at a scan rate of 100 mV/s between −0.2 and 1.6 V in 0.5 M H_2SO_4 until a stable CV curve was obtained.

For the single-signal sensor configuration, the cleaned electrodes were dipped in 50 μL of 0.5 μM capture DNA containing 0.2 mM TCEP for 12 h at room temperature to obtain c-DNA/GE. The capture DNA-modified electrode was blocked to reduce nonspecific binding by soaking in 1 mM MCH for 30 min (MCH/c-DNA/GE). Subsequently, the modified electrodes were immersed in some 50 μL of solutions containing different concentrations of target DNA−reporter complexes and incubated for 1 h at 37 °C. These target DNA−reporter complexes first were prepared through incubation of different concentration target DNA with 2 μM reporter DNA for 5 min at 90 °C in a water bath and hybridization overnight after naturally cooling to room temperature. Finally, 10 μL of SA-HRP was dropped onto the modified electrode and allowed to rest for 1 h. After each step, the electrode was thoroughly rinsed with ultrapure water in order to minimize physical adsorption and nonspecific interactions on the GE. Amperometric detection was then performed in 0.1 M PBS (pH 5.0) containing 30% H_2O_2 and 10 μL of TMB. Reproducibility was characterized by repeating measurements with at least three equivalently prepared electrodes.

For the double-signal sensor configuration, cleaned electrodes were dipped in 0.2 mM TCEP containing hairpin DNA for 12 h at room temperature to obtain SH-DNA-Fc/GE. Nonspecific sites on the SH-DNA-Fc/GE were blocked in 1 mM MCH for 30 min (MCH/SH-DNA-Fc/GE). The electrode was prepared for SWV detection in 0.1 M PBS (pH = 7.4). The modified electrode was then immersed in some 50 μL of solutions containing different concentrations of target DNA−reporter complexes and incubated for 1 h at 37 °C (RP-DNA/T-DNA/MCH/SH-DNA-Fc/GE). SWV was again performed in 0.1 M PBS (pH 7.4). The target DNA−reporter complexes were prepared by same method as above. Finally, 10 μL of SA-HRP was dropped onto the modified electrode and allowed to rest for 1 h. After each step, the electrode was thoroughly rinsed in ultrapure water to minimize physical adsorption and nonspecific interactions at the GE. Amperometric detection was finally performed in 0.1 M PBS (pH 5.0) containing 30% H_2O_2 and 10 μL of TMB. The reproducibility of the biosensor was verified by repeating measurements with at least three equivalently prepared electrodes.

Electrochemical Measurement. All electrochemical measurements including CV, EIS, SWV, and amperometry were performed with a conventional three-electrode system. CV was performed in 0.1 M KCl containing 1 mM $K_3[Fe(CN)_6]$ at a scan rate of 100 mV/s in the potential range from −0.2 to 0.6 V. All EIS spectra were obtained using ac modulation in the frequency range from 0.01 Hz to 100 kHz in 0.5 M KNO_3 containing 0.5 mM $K_3[Fe(CN)_6]/K_4[Fe(CN)_6]$ (1:1). SWV was performed in 10 mM PBS in the potential range from 0 to 0.7 V with a modulation amplitude of 4 mV, a step potential of 25 mV, and a frequency of 25 Hz. Amperometric detection was performed at 150 mV, and the electrochemical reduction current was measured 100 s after the SA-HRP redox reaction reached steady state.

RESULTS AND DISCUSSION

Design Principle of the Sensors. The single-signal sensor was first designed with only the HRP reporter for the detection

DOI: 10.1021/acsami.7b15014
ACS Appl. Mater. Interfaces 2017, 9, 44231−44240

Scheme 1. Schematic Diagram of Electrochemical DNA Biosensor for d(CAG)$_n$ TNRs Based on Enzyme-Catalyzed Amplification (Single-Signal Biosensor)

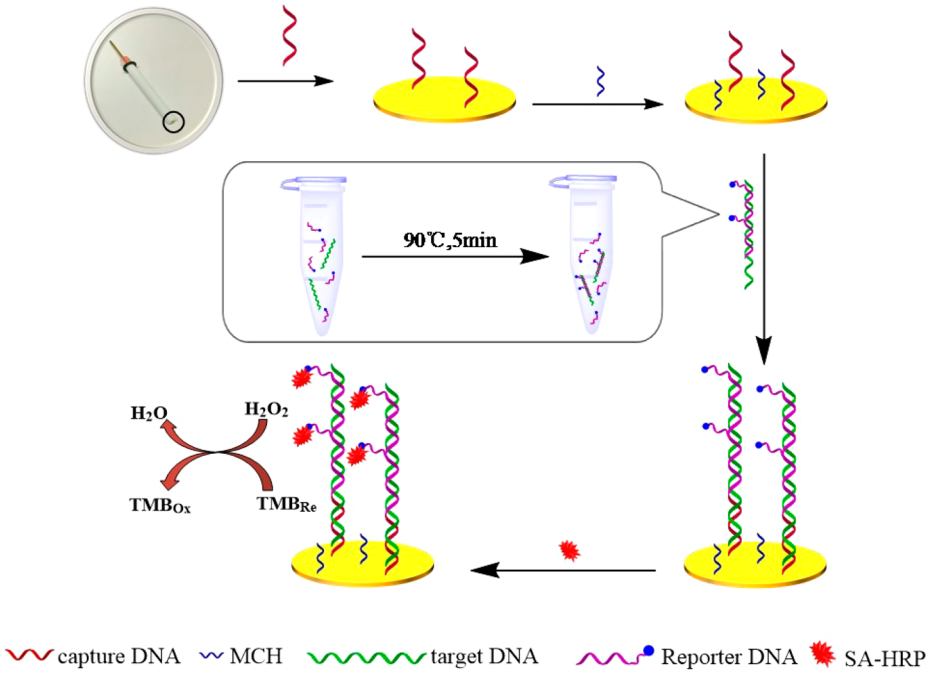

of d(CAG)$_n$ TNRs, as shown in Scheme 1. Capture DNA was immobilized at the GE surface via gold−sulfur (Au−S) bonds. The hybridization complex of target DNA and reporter DNA was modified on the electrode surface through the hybridization of 3′ terminus region of the sequence and capture DNA sequence.

During hybridization reaction, different sequence hybridizations were used for capture, target, and reporter DNA. Typically, a multistep DNA-modified electrode was hybridized step-by-step. In this approach, the universal hybridization process was used based on a previous study. Target DNA was first hybridized to a capture DNA-modified electrode. Reporter DNA was then added through incubation with SA-HRP. In this hybridization mode, unsatisfactory results were obtained. The desired signal was not achieved, especially in terms of its sensitivity to repeat length. It was contributed to the formation of hairpin secondary of d(CAG)$_n$ TNR, which was more stable with increasing the length of repeat.[24,25]

Here, we changed the order of hybridization. Considering the form of secondary structure particularity of d(CAG)$_n$ TNR, the use of a higher hybridization temperature was beneficial for achieving the desired hybridization complex of d(CAG)$_n$ and reporter-DNA. Normally, two single strands were hybridized at approximately 37 °C. Indeed, we found that target DNA did not successfully hybridize with reporter DNA at 37 °C. Even at 65 °C hybridization was unstable. Because of the high propensity of target d(CAG)$_{35}$ to form a stable hairpin structure, hybridization was performed by heating the sample at 90 °C for 5 min and allowing it to cool to room temperature. This method resulted in a more complete hybridization of target DNA with the short reporter DNA. Continually capture DNA on the electrode surface hybridized to the target DNA with a short strand of reporter DNA at 37 °C. SA-HRP was then bound to the working electrode through strong biotin−avidin interactions. Finally, i−t curves were measured for the electrocatalytic reaction. In the absence of target DNA, SA-HRP was not bound to the modified electrode, and the biosensor was not effective.

DNA hairpin molecular beacons, which exhibit a higher selectivity for SNPs than linear DNA based on thermodynamic considerations when used in fluorescent molecular beacons, have been used successfully for electrochemical label-free DNA detection.[26−28] Electrochemical molecular beacons alter the efficiency of electron transfer (ET) between the electrode and redox labels placed further from the electrode in the hybridized (open) beacon state. The process can then be detected electrochemically based on a calibration of signal vs the concentration of capture DNA.

In this work, the electrochemical molecular beacon with ferrocene was used to create a new electrochemical sensor based on a double-signal technique in which ferrocene acted as a label of electrochemical molecular beacon and HRP acted as label of short reporter DNA. This double-signal technique was created to mainly improve length detection for d(CAG)$_n$ TNRs. As shown in Scheme 2, hairpin molecular beacons labeled with ferrocene, instead of single DNA with no label, was used as capture DNA. Hairpin DNA (SH-DNA-Fc) was also modified via Au−S bonding. The hybridization of target DNA and short reporter DNA was performed as described in Scheme 1. When hairpin DNA on the surface of the electrode hybridized with a hybridization complex of target DNA and reporter DNA, the hairpin DNA can open, resulting in a decreased signal from the ET of ferrocene (F represent the ferrocene signal changes). Similarly, SA-HRP was bound to the working electrode, producing a signal from HRP catalytic redox of TMB (H). The relative length of the repeat can be calculated from the ratio of the electrochemical signal intensities of the hybridized RP-DNA (HRP-linked assay) and the molecular beacon (ferrocene label).

Characterization of the DNA Biosensor. Among the available electrochemical techniques, EIS is used most often to study surface processes and properties,[29−31] e.g., molecular binding processes. EIS is a powerful tool for monitoring surface processes at electrodes and studying DNA hybridization,[32−36] protein−DNA interactions,[37,38] and antigen−antibody recognition.[39]

DOI: 10.1021/acsami.7b15014
ACS Appl. Mater. Interfaces 2017, 9, 44231−44240

Scheme 2. Schematic Diagram of Double-Signal Biosensor for Measuring the Sequence and Length of d(CAG)$_n$ TNRs[a]

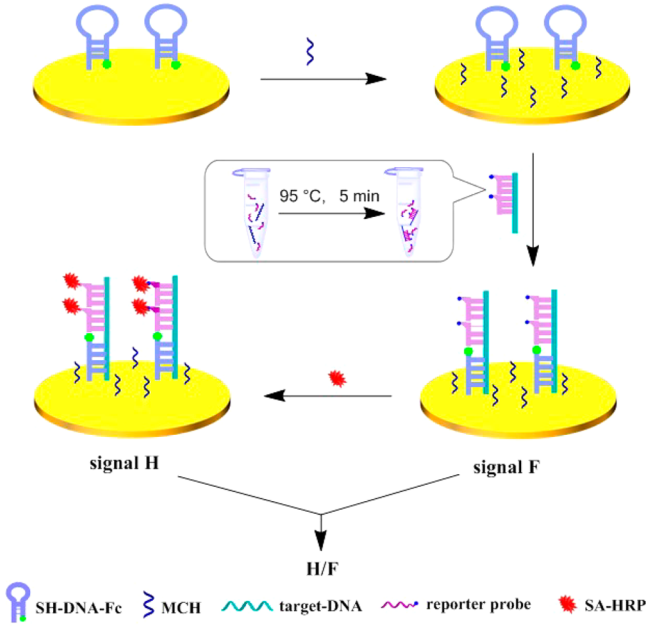

[a]F is the signal change from ferrocene, and H is the signal from the HRP-catalyzed reaction.

Here, self-assembly at the electrochemical sensor was investigated using EIS. As shown in Figures 1A and 1B, $[Fe(CN)_6]^{3-}/[Fe(CN)_6]^{4-}$ was used as the redox probe in the frequency range from 0.01 Hz to 10 kHz. The electron-transfer resistance (R_{et}) of the bare GE was very small, as demonstrated by the nearly straight line (curve a) in Figure 1A. After the immobilization of capture DNA on the electrode via Au−S bonding, the impedance increased significantly (curve b) compared to that of the bare GE. After blocking with MCH, R_{et} increased more (curve c). When the modified GE was immersed in 2 μM of the hybridized complex of RP-DNA and different concentrations of target DNA, R_{et} increased significantly (curve d). Overall, these results indicated the successful preparation of the desired electrochemical sensor, which provided a sensitive sensing platform for CAG TNRs.

The self-assembly of the DNA biosensor was investigated using CV. As shown in Scheme 1 and Figure 1C, the bare GE exhibited reversible redox peaks (curve a). After capture DNA was self-assembled on the bare GE surface, the redox current decreased (curve b) because of electronic repulsion between $Fe(CN)_6^{4-/3-}$ and the negatively charged DNA backbones. The redox current continued to decrease (curve c) when unoccupied sites on the sensor's surface were blocked with MCH. After the hybridized complex of target DNA and RP-DNA was captured, the peak current decreased and the difference in the peak potentials increased (curve d). These results were consistent with those of EIS, again verifying the successful preparation of the biosensor as a sensitive sensing platform for d(CAG)$_n$ TNRs.

As shown in Scheme 2, when the capture DNA (hairpin DNA) was assembled on the surface of the electrode, the ferrocene label was very close to the electrode surface, resulting in a high current for ferrocene redox reactions. This was confirmed experimentally, as shown in Figure 1D. A clear current peak was observed for ferrocene (curve a) after the surface was modified with hairpin DNA. After the complex of T-DNA and RP-DNA were added, the current decreased (curve b) because the ferrocene label became farther away from the surface of the electrode after the hairpin DNA opened. In addition, some control experiments were performed as shown in Figure S2. When the part sequence of target DNA do not match with hairpin DNA, the signal of ferrocene

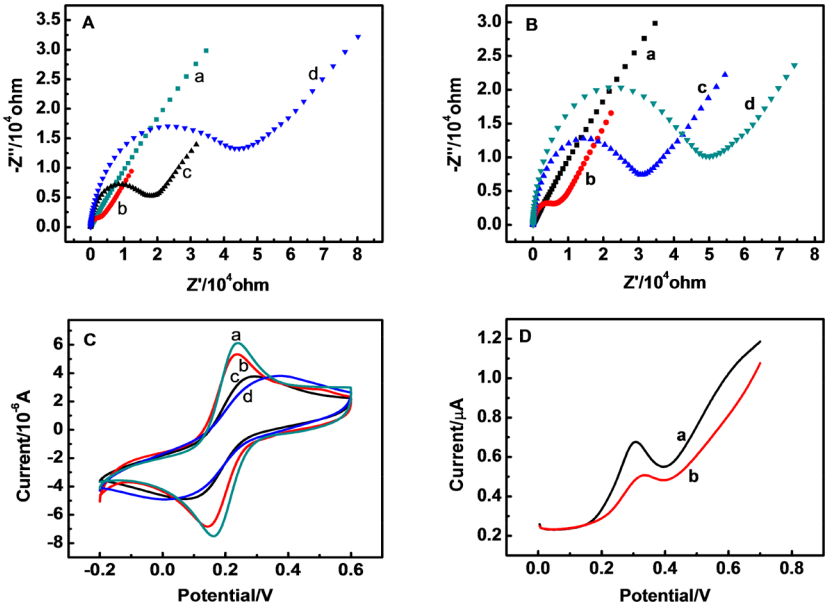

Figure 1. (A, B) Nyquist plots for the progressively modified sensors depicted for single-signal biosensor (A) and double-signal biosensor (B) in 0.5 mM $Fe(CN)_6^{3-/4-}$, respectively. In (A) the points correspond to the (a) bare GE, (b) c-DNA/GE, (c) MCH/c-DNA/GE, and (d) RP-DNA/T-DNA/MCH/c-DNA/GE. In (B) the points correspond to the (a) bare GE, (b) SH-DNA-Fc/GE, (c) MCH/SH-DNA-Fc/GE, and (d) RP-DNA/T-DNA/MCH/SH-DNA-Fc/GE. (C) CV of the progressively modified sensor described in Scheme 1 in 0.5 mM $Fe(CN)_6^{3-/4-}$ at a (a) bare GE, (b) c-DNA/GE, (c) MCH/c-DNA/GE, and (d) RP-DNA/T-DNA/MCH/c-DNA/GE. (D) SWV curves of (a) SH-DNA-Fc/GE in PBS (pH 7.4) after the surface was modified with hairpin DNA and (b) RP-DNA/T-DNA/MCH/SH-DNA-Fc/GE in PBS (pH 7.4) after the hairpin DNA was hybridized with a complex of T-DNA and RP-DNA for 1 h.

DOI: 10.1021/acsami.7b15014
ACS Appl. Mater. Interfaces 2017, 9, 44231−44240

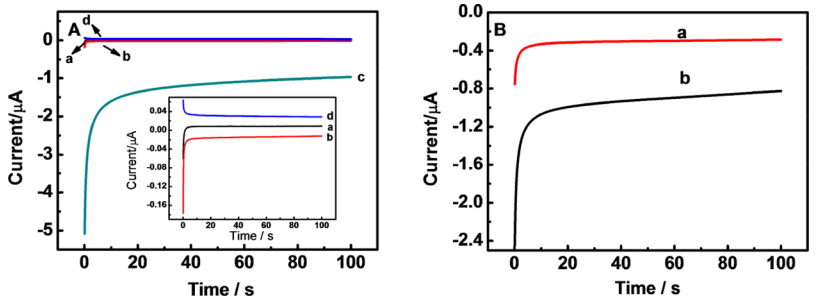

Figure 2. (A) Amperometric responses after 30 min incubation for the (a) SA-HRP/T-DNA/MCH/c-DNA/GE, (b) SA-HRP/RP-DNA/MCH/c-DNA/GE, (c) SA-HRP/RP-DNA/T-DNA/MCH/c-DNA/GE, and (d) RP-DNA/T-DNA/MCH/c-DNA/GE. (B) Amperometric responses after 30 min incubation for (a) SA-HRP/RP-DNA/MCH/SH-DNA-Fc/GE and (b) SA-HRP/RP-DNA/T-DNA/MCH/SH-DNA-Fc/GE. Amperometric detection was performed in 0.1 M PBS containing 10 μL of H_2O_2 and 10 μL of TMB.

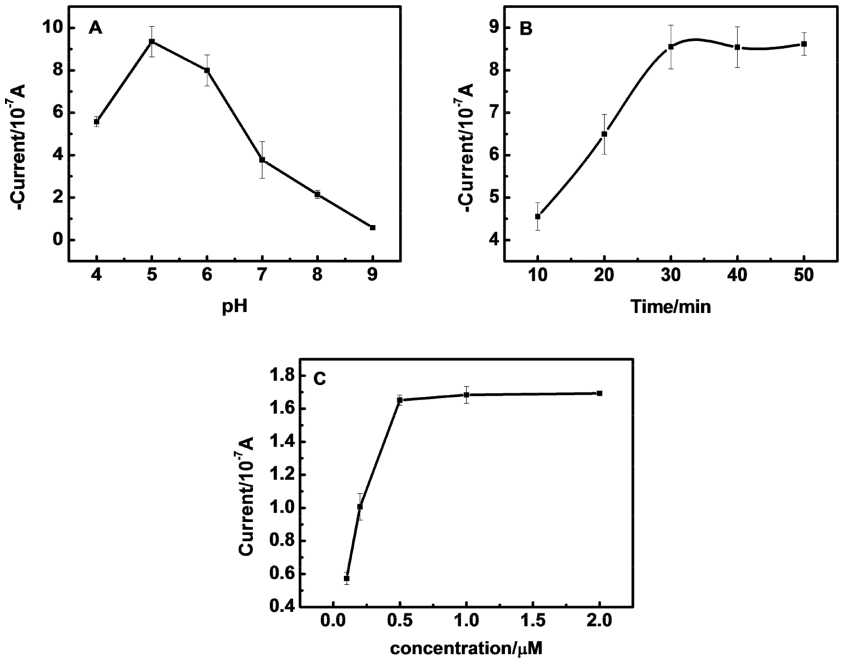

Figure 3. (A) Effect of buffer pH on the current for the electrochemical sensor. (B) Effect of the binding time between SA-HRP and RP-DNA. The target DNA concentration was 100 pM. (C) Ferrocene current at different concentrations of SH-DNA-Fc in the electrochemical sensor.

was almost no change because of no good hybridization (curve c). If the capture DNA is not hairpin DNA, the signal of ferrocene is lower because it is far away the electrode surface (curve d).

Detection at the Electrochemical Sensor. In this work, HRP was captured on the surface of the electrode during the last sensing step via biotin−streptavidin binding between SA-HRP and RP-DNA. The electrochemical signal was generated through reduction of TMB_{ox} by HRP catalyzed H_2O_2. The signal was measured to further confirm hybridization and successful sensor construction. To investigate improvements in sensing as a result of adding SA-HRP, the amperometric responses of different modified electrodes were recorded, as shown in Figure 2A. For example, in the absence of RP-DNA or target DNA (Scheme 1), only a negligible amperometric current was observed (Figure 2A, curves a and b) because SA-HRP was not bound to the biosensor's surface. In the absence of SA-HRP, the electrochemical reaction was not catalyzed (curve d). After hybridization and the binding of SA-HRP, the amperometric signal increased to 969 nA (curve c), which was 70 times higher than the current (12.2 nA) without target DNA (curve b). In the double-signal sensor, only a very small amperometric current was observed in the absence of target DNA (Figure 2B, curve a). Importantly, the amperometric response increased in the presence of target DNA (curve b), indicating that both the single- and double-signal sensors exhibited excellent signals for the detection of $d(CAG)_n$ TNRs.

Optimization of Assay Conditions. The detection of $d(CAG)_n$ TNRs in these sensors was based on long-range self-assembled DNA nanostructures and the use of appropriate binding conditions. As described above, the choice of hybridization sequence and temperature was very important for achieving good performance. During experiments, electrochemical signals were found to be closely related to the pH value of the test solution and the binding time of SA-HRP with biotin. As shown in Figure 3A, the current response was at peak about pH 5.0. The effect of the binding time between SA-HRP and biotin was also examined, as shown in Figure 3B. The electrochemical signal increased as the binding time increased from 0 to 30 min before reaching a constant value. Therefore, a binding time of 30 min was chosen as the optimum value for long-range self-assembly.

For double-signal sensor, the choice of electrochemical molecular beacon was very important for determining overall performance. The ferrocene signal was strongly dependent on the

DOI: 10.1021/acsami.7b15014
ACS Appl. Mater. Interfaces 2017, 9, 44231−44240

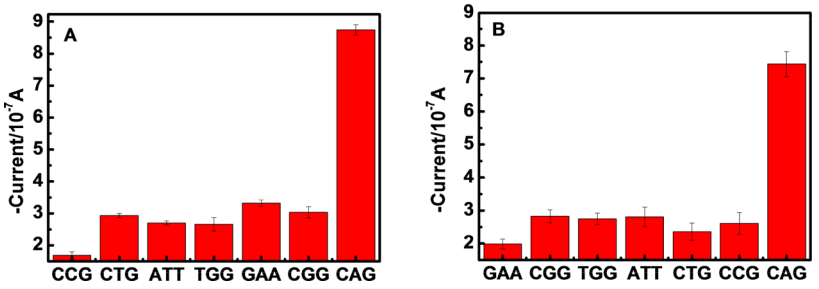

Figure 4. Selectivity of single-signal sensor (A) and double-signal sensor (B) for CAG TNRs (100 pM) and of other interfering TNRs (1 nM).

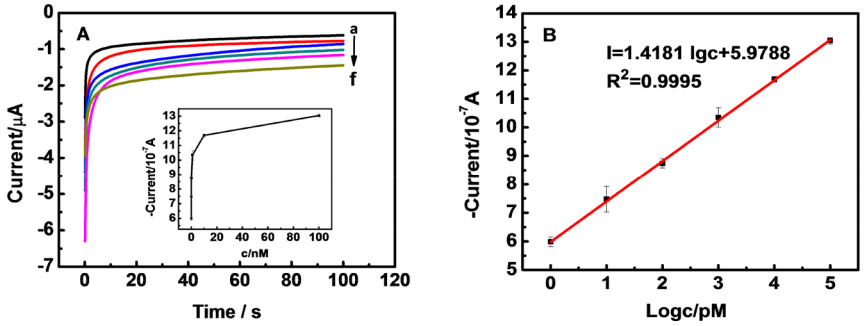

Figure 5. (A) Current responses from HRP catalyzed redox in single-signal sensor that was incubated in different concentrations (a to f: 1, 10, 100, 1000, 10 000, and 100 000 pM) of CAG TNRs in PBS (pH 5.0). Inset: current vs DNA concentration. (B) Calibration curve for current vs the logarithm of the d(CAG)$_n$ TNR concentration. Error bars indicate standard deviations of three measurements.

concentration of SH-DNA-Fc. As shown in Figure 3C, the ferrocene signals increased as the concentration was increased from 0.1 to 0.5 μM. Above 0.5 μM, the signal did not increase further. Therefore, a SH-DNA-Fc concentration of 0.5 μM was chosen as the optimum concentration for long-range self-assembly.

Selectivities of the Electrochemical Sensors. A sufficient signal is required for a useful electrochemical sensor, which was certificated by above measurements. Selectivity is a critical property of a useful biosensor. In both single- and double-signal sensors, obtaining a good selectivity for different TNRs was a primary concern. To evaluate the selectivities of the proposed sensors, several interfering TNRs that was associated with neurodegenerative diseases were tested, including d(CCG)$_{15}$, d(CTG)$_{15}$, d(ATT)$_{15}$, d(TGG)$_{15}$, d(GAA)$_{15}$, and d(CGG)$_{15}$. A comparative study was performed by measuring a low concentration of target DNA (100 pM) and a high concentration of interfering species (1 nM). The amperometric responses of d(CAG)$_n$ TNRs and others interfering DNA strands are shown in Figure S1 and are summarized in Figure 4. The highest current was observed for the (CAG)$_n$ TNR even if the concentration of (CAG)$_n$ was only 1/10 concentration of interfering species. These results clearly demonstrated the high selectivity of both the single- and double-signal sensors for d(CAG)$_n$ among TNR biomarkers of neurodegenerative diseases.

Effect of Target DNA on Signals from Ferrocene and HRP. The relationship between output signal and the concentration of target DNA was investigated for the quantitative detection of d(CAG)$_n$ TNRs. The single-signal sensor was tested first. Amperometric i−t curves were obtained under optimal experimental conditions. The electrochemical signal from HRP catalyzed redox increased when the concentration of d(CAG)$_n$ increased until a signal plateau was reached. As shown in Figure 5A, the amperometric current increased with the concentration of target DNA from 1 pM to 100 nM. The current (I) vs the logarithm of target DNA concentration (c) exhibited a linear relationship, where $I = 1.4181 \log(c) + 5.9788$ with a correlation coefficient of 0.9995 (Figure 5B). The LOD was 0.21 pM (LOD = $3\sigma/k$ where σ is the standard deviation of the blank and k is the slope of the calibration curve[40]).

For double-signal sensor, the linearity of the ferrocene and HRP signals with d(CAG)$_n$ repeat concentration was tested. Amperometric i−t curves were obtained in the presence of different concentrations of d(CAG)$_n$ TNRs (Figure 6A). Clearly, the HRP portion of the sensor was very sensitive to concentration from 1 pM to 10 nM, and its signal continued to increase slowly as the concentration was increased up to 100 nM. The I vs $\log(c)$ plot was linear with $I = 1.20599 \log(c) + 4.93149$ and a correlation coefficient of 0.9993 (Figure 6B). The LOD was 0.15 pM.

To evaluate the opening of the electrochemical molecular beacon, SWV curves were measured for ferrocene after the capture DNA-modified electrodes were incubated with the hybridized complex of d(CAG)$_n$ and RP-DNA. The change in current ($\Delta I = I_0 - I_c$, where I_0 is the current response in the folded state before incubation with target DNA and I_c is the current response in the open state after incubation with different concentrations of target DNA) was measured as a function of d(CAG)$_n$ concentration. As shown in Figure 6C, ΔI increased with increasing concentration of target DNA until a stable state was reached. A linear regression equation was fit to the results such that $\Delta I = 0.11576 \log(c) + 0.356$ with a correlation coefficient of 0.997 (Figure 6D). The LOD was 0.26 pM.

Overall, these results indicated that the responses of both sensors exhibited excellent quantitative correlations with the concentration of target DNA. LOD and sensitivity were greatly improved compared to those achieved in previous work.[2,15,18,19] In addition, the sensors have also better sensitivity and lower LOD in comparison with other work (Table S1).

Relationship between Repeat Number and Current. Although TNRs are significant biomarkers for the early diagnosis of neurodegenerative diseases, the detection of specific

DOI: 10.1021/acsami.7b15014
ACS Appl. Mater. Interfaces 2017, 9, 44231−44240

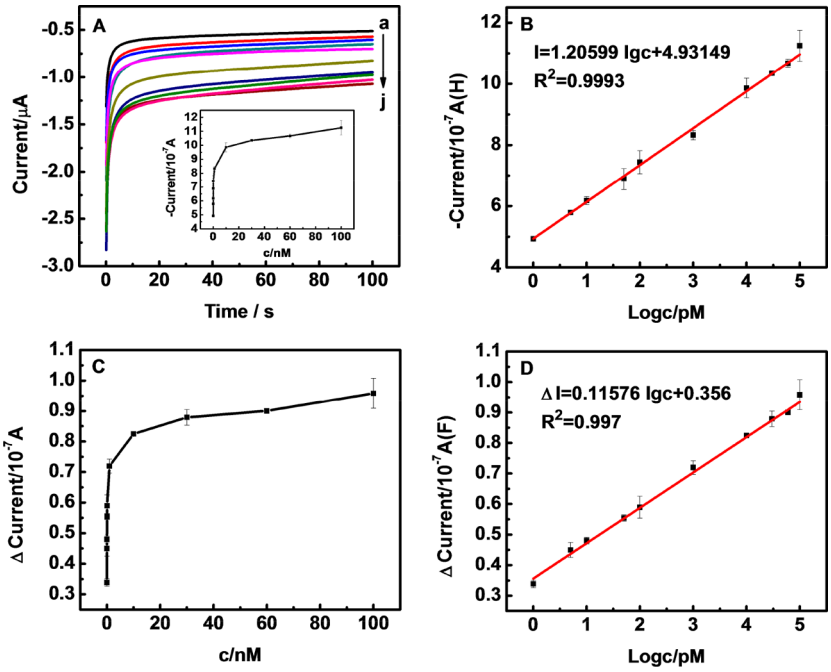

Figure 6. (A) Amperometric responses from HRP catalyzed redox in double-signal sensor that was incubated in different CAG TNR concentrations (a to j: 0.001, 0.005, 0.01, 0.05, 0.1, 1, 10, 30, 60, and 100 nM) in PBS (pH 5.0). Inset: current vs DNA concentration. (B) Calibration curve for current vs the logarithm of CAG TNR concentration. Error bars indicate the standard deviations of three measurements. (C) SWV responses of ferrocene after the electrode was incubated in different CAG TNR concentrations in PBS (pH 5.0). (D) Calibration curve for current vs the logarithm of CAG TNR concentration. Error bars represent the standard deviations of three measurements.

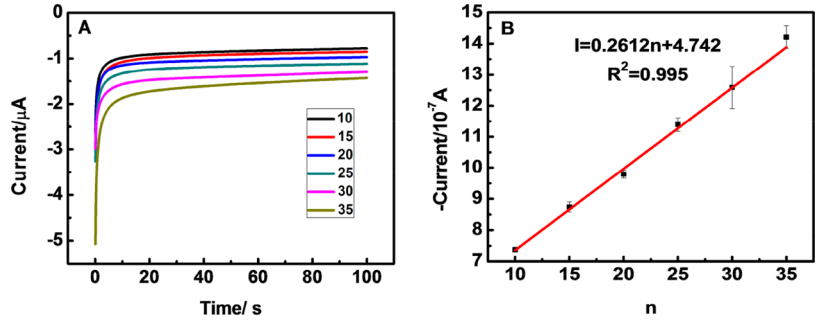

Figure 7. (A) Current responses from HRP catalyzed redox in single-signal sensor that was incubated with CAG TNRs with different numbers of repeats (n = 10, 15, 20, 25, 30, and 35) in PBS (pH 5.0). (B) Linear relationship between steady-state current and n at a DNA concentration of 100 pM. Error bars represent the standard deviations of three measurements.

sequences of TNRs has received little attention from researchers. Repeat number is particularly difficult to measure, although this information is extremely important for diagnosing neurodegenerative diseases.[41] In this work, double-signal sensor was specifically designed for the more reliable determination of repeat number.

The effect of repeat number on the current from HRP catalyzed redox in single-signal sensor was considered first. $d(CAG)_n$ at a concentration of 100 pM and with different numbers of repeats (n = 10−35) was measured at the single-signal sensor. As shown in Figure 7A, the amperometric current increased when n increased. A linear relationship was observed between current and n (I = 0.2612n + 4.742) with a correlation coefficient of 0.995 (Figure 7B).

Despite the linear correlation between the signal and n for single-signal sensor at some concentration, the electrochemical signal increased with increasing concentration of repeats, as shown in Figure 5 (single-signal sensor). So, it is unreliable and unscientific that the n value was determined by the method. In order to further improve reliability and stability, double-signal sensor containing two variables was developed. As shown in Scheme 2 and Figure 1D, only when one strand of the target repeat was captured on the surface of the electrode did the electrochemical molecular beacon open, leading to a change in the ferrocene signal. Consequently, there was a clear and direct relationship between the change in the ferrocene signal and the number of $d(CAG)_n$ strands. Meanwhile, the repeat number is more, and more RP-DNA can bind to a single target DNA, resulting in a higher signal for HRP. Therefore, the ratio of the signals (H/F) from HRP catalyzed redox and ferrocene was used as a metric for n to improve the accuracy and stability of repeat length measurements.

As shown in Figures 6B and 6D, $d(CAG)_{15}$ was used to determine the effect of concentration on H and F. H and F increased linearly with the logarithm of concentration, but the slope of H vs log(c) was larger than that of F vs log(c), as shown in the inset to Figure 8. H/F was calculated for each individual

DOI: 10.1021/acsami.7b15014
ACS Appl. Mater. Interfaces 2017, 9, 44231−44240

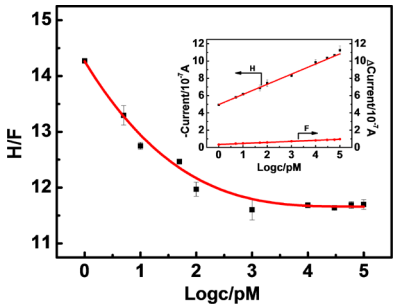

Figure 8. H/F at different $d(CAG)_{15}$ TNR concentrations. Inset: H vs $\log(c)$ had a larger slope than F vs $\log(c)$.

sample at different concentrations. As shown in Figure 8, H/F was approximately constant at target DNA concentrations between 1 and 100 nM, indicating that repeat length can be measured over a low and wide concentration range. A target concentration of 10 nM was used for further investigations.

The effect of repeat number on the hybridization signal was investigated. $d(CAG)_n$ TNRs with different values of n were bound to RP-DNA. As shown in Figure 9A, the current change of ferrocene (F) remained relatively stable with increasing n at the same target concentration. In contrast, the current from HRP catalyzed redox (H) increased obviously with increasing n (Figure 9B). H increased faster than F, as shown in Figure 9C. A linear relationship ($H/F = 0.1398n + 9.89788$) with a correlation coefficient of 0.974 was observed between H/F and n (Figure 9D). The number of TNRs was reliably obtained from measurements of H/F using this double-signal technique, which should be useful for the early diagnosis of neurodegenerative diseases via a simple, rapid, and inexpensive electrochemical sensor.

CONCLUSION

In this work, we developed a new double-signal technique based on a simple and sensitive electrochemical biosensor for the highly selective and accurate detection of the sequence and length of a CAG TNR. In the technique, an electrochemical molecular beacon labeled with ferrocene was used to capture CAG TNR strands that were also hybridized to a short reporter DNA strand labeled with HRP. SWV was used to measure ferrocene, and amperometric i–t curves were obtained to investigate the function of this new electrochemical biosensor. The proposed strategy sensitively and selectively detected CAG TNRs from 1 pM to 100 nM with a LOD 0.15 pM. Importantly, the signal ratio, H/F, was used as the metric for obtaining a reliable repeat number-dependent signal in the double-signal technique, and only 10 nM target DNA was required. The linear equation $H/F = 0.1398n + 9.89788$ (n = 10–35) was obtained with a correlation coefficient of 0.974. In addition, this procedure was suitable for the detection of CAG TNRs and can also be used to detect other TNRs. This new double-signal electrochemical biosensor provides a feasible strategy to determine the sequence and length of CAG TNRs in clinical applications, suggesting promising new strategies for the early diagnosis of neurodegenerative diseases.

ASSOCIATED CONTENT

Supporting Information

The Supporting Information is available free of charge on the ACS Publications website at DOI: 10.1021/acsami.7b15014.

Detailed supplementary methods, DNA sequence, Table S1, and Figures S1 and S2 (PDF)

AUTHOR INFORMATION

Corresponding Authors

*(H.H.) Tel +86-027-50865319; fax +86-027-88663043; e-mail hehanping@hubu.edu.cn.

*(G.C.) Tel +86-027-50865319; fax +86-027-88663043; e-mail changgang@hubu.edu.cn.

ORCID

Hanping He: 0000-0002-7078-3245

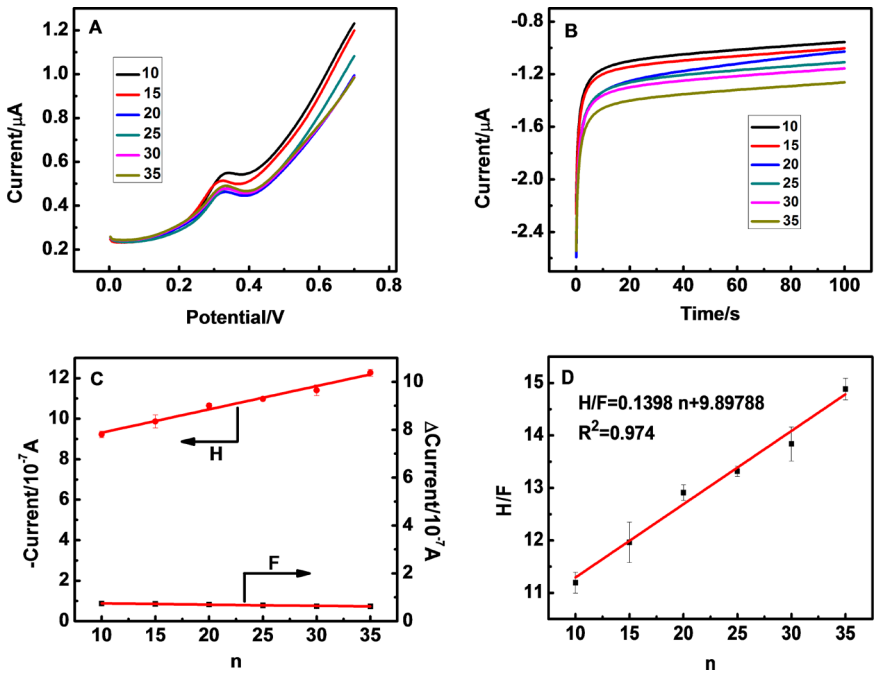

Figure 9. (A) SWV curves for ferrocene at different repeat numbers. (B) Amperometric responses from catalyzed HRP redox at different repeat numbers. (C) Histogram of H and F at different repeat numbers. (D) The corresponding calibration curve of H/F vs n. All experiments were performed in PBS (pH = 5.0). Values are the average of three samples.

DOI: 10.1021/acsami.7b15014
ACS Appl. Mater. Interfaces 2017, 9, 44231–44240

Notes

The authors declare no competing financial interest.

■ ACKNOWLEDGMENTS

This work was supported by the National Natural Science Foundation of China (Grant 21575035) and Foreign Science and Technology Cooperation Fund of Hubei province, China (2015BHE025).

■ REFERENCES

(1) Volle, C. B.; Delaney, S. CAG/CTG Repeats Alter the Affinity for the Histone Core and the Positioning of DNA in the Nucleosome. *Biochemistry* **2012**, *51*, 9814−9825.
(2) He, H. P.; Xia, J. P.; Peng, X. Q.; Chang, G.; Zhang, X. H.; Wang, Y. F.; Nakatani, K.; Lou, Z. W.; Wang, S. F. Facile Electrochemical Biosensor Based on a New Bifunctional Probe for Label-free Detection of CGG Trinucleotide Repeat. Biosens. *Biosens. Bioelectron.* **2013**, *49*, 282−289.
(3) McMurray, C. T. Mechanisms of Trinucleotide Repeat Instability during Human Development. *Nat. Rev. Genet.* **2010**, *11*, 786−799.
(4) Kozlowski, P.; de Mezer, M.; Krzyzosiak, W. J. Trinucleotide Repeats in Human Genome and Exome. *Nucleic Acids Res.* **2010**, *38*, 4027−4039.
(5) Lopez, C. A.; Cleary, J. D.; Pearson, C. E. Repeat Instability as the Basis for Human Diseases and as a Potential Target for Therapy. *Nat. Rev. Mol. Cell Biol.* **2010**, *11*, 165−170.
(6) Mirkin, S. M. Expandable DNA Repeats and Human Disease. *Nature* **2007**, *447*, 932−940.
(7) Pearson, C. E.; Edamura, K. N.; Cleary, J. D. Repeat Instability: Mechanisms of Dynamic Mutations. *Nat. Rev. Genet.* **2005**, *6*, 729−742.
(8) Ross, C. A.; Tabrizi, S. J. Huntington's Disease: From Molecular Pathogenesis to Clinical Treatment. *Lancet Neurol.* **2011**, *10*, 83−98.
(9) Walker, F. O. Huntington's Disease. *Lancet* **2007**, *369*, 218−228.
(10) Barros, S. A.; Chenoweth, D. M. Triptycene-based Small Molecules Modulate (CAG)-(CTG) Repeat Junctions. *Chem. Sci.* **2015**, *6*, 4752−4755.
(11) Huang, J.; Delaney, S. Unique Length-Dependent Biophysical Properties of Repetitive DNA. *J. Phys. Chem. B* **2016**, *120*, 4195−4203.
(12) Lin, M. H.; Wang, J. J.; Zhou, G. B.; Wang, J. B.; Wu, N.; Lu, J. X.; Gao, J. M.; Chen, X. Q.; Shi, J. Y.; Zuo, X. L.; Fan, C. H. Programmable Engineering of a Biosensing Interface with Tetrahedral DNA Nanostructures for Ultrasensitive DNA Detection. *Angew. Chem.* **2015**, *127*, 2179−2183.
(13) Kannan, B.; Williams, D. E.; Booth, M. A.; Travas-Sejdic, J. Highsensitivity, Label-Free DNA Sensors Using Electrochemically Active Conducting Polymers. *Anal. Chem.* **2011**, *83*, 3415−3421.
(14) Boal, A. K.; Barton, J. K. Electrochemical Detection of Lesions in DNA. *Bioconjugate Chem.* **2005**, *16*, 312−321.
(15) He, H. P.; Peng, X. Q.; Huang, M.; Chang, G.; Zhang, X. H.; Wang, S. F. An Electrochemical Impedance Sensor Based on a Small Molecule Modified Au Electrode for the Recognition of a Trinucleotide Repeat. *Analyst* **2014**, *139*, 5482−5487.
(16) Yuan, R.; Ding, S. J.; Yan, Y. R.; Zhang, Y.; Zhang, Y. H.; Cheng, W. A Facile and Pragmatic Electrochemical Biosensing Strategy for Ultrasensitive Detection of DNA in Real Sample Based on Defective T Junction Induced Transcription Amplification. *Biosens. Bioelectron.* **2016**, *77*, 19−25.
(17) Yang, L. L.; Tao, Y. Z.; Yue, G. Y.; Li, R. B.; Qiu, B.; Guo, L. H.; Lin, Z. Y.; Yang, H. H. Highly Selective and Sensitive Electrochemiluminescence Biosensor for p53 DNA Sequence Based on Nicking Endonuclease Assisted Target Recycling and Hyperbranched Rolling Circle Amplification. *Anal. Chem.* **2016**, *88*, 5097−5103.
(18) He, H. P.; Xia, J. P.; Chang, G.; Peng, X. Q.; Lou, Z. W.; Nakatani, K.; Zhou, X.; Wang, S. F. Selective Recognition of G-G Mismatch Using the Double Functional Probe with Electrochemical Active Ferrocenyl. *Biosens. Bioelectron.* **2013**, *42*, 36−40.
(19) Li, J.; He, H. P.; Peng, X. Q.; Huang, M.; Zhang, X. H.; Wang, S. F. Electrochemical Investigation of Interaction between a Bifunctional Probe and GG Mismatch Duplex. *Anal. Sci.* **2015**, *31*, 663−667.
(20) Kamada, K.; Nakamura, T.; Tsukahara, S. Photoswitching of Enzyme Activity of Horseradish Peroxidase Intercalated into Semiconducting Layers. *Chem. Mater.* **2011**, *23*, 2968−2972.
(21) Liu, G.; Wan, Y.; Gau, V.; Zhang, J.; Wang, L. H.; Song, S. P.; Fan, C. H. An Enzyme-Based E-DNA Sensor for Sequence-Specific Detection of Femtomolar DNA Targets. *J. Am. Chem. Soc.* **2008**, *130*, 6820−6825.
(22) Patolsky, F.; Lichtenstein, A.; Willner, I. Detection of Single-base DNA Mutations by Enzyme-Amplified Electronic Transduction. *Nat. Biotechnol.* **2001**, *19*, 253−257.
(23) Yu, C. J.; Wan, Y. J.; Yowanto, H.; Li, J.; Tao, C. L.; James, M. D.; Tan, C. L.; Blackburn, G. F.; Meade, T. J. Electronic Detection of Single-Base Mismatches in DNA with Ferrocene-Modified Probes. *J. Am. Chem. Soc.* **2001**, *123*, 11155−11161.
(24) Paiva, A. M.; Sheardy, R. D. The Influence of Sequence Context and Length on the Kinetics of DNA Duplex Formation from Complementary Hairpins Possessing (CNG) Repeats. *J. Am. Chem. Soc.* **2005**, *127*, 5581−5585.
(25) Degtyareva, N. N.; Barber, C. A.; Sengupta, B.; Petty, J. T. Context dependence of trinucleotide repeat structures. *Biochemistry* **2010**, *49*, 3024−3030.
(26) Bonnet, G.; Tyagi, S.; Libchaber, A.; Kramer, F. R. Thermodynamic Basis of the Enhanced Specificity of Structured DNA Probes. *Proc. Natl. Acad. Sci. U. S. A.* **1999**, *96*, 6171−6176.
(27) Tyagi, S.; Kramer, F. R. Molecular Beacons: Probes that Fluoresce upon Hybridization. *Nat. Biotechnol.* **1996**, *14*, 303−308.
(28) Tsourkas, A.; Behlke, M. A.; Rose, S. D.; Bao, G. Hybridization Kinetics and Thermodynamics of Molecular Beacons. *Nucleic Acids Res.* **2003**, *31*, 1319−1330.
(29) Bardea, A.; Patolsky, F.; Dagan, A.; W illner, I. Sensing and Amplification of Oligonucleotide-DNA Interactions by Means of Impedance Spectroscopy: a Route to a Tay−Sachs Sensor. *Chem. Commun.* **1999**, 21−22.
(30) Katz, E.; Willner, I. Probing Biomolecular Interactions at Conductive and Semiconductive Surfaces by Impedance Spectroscopy: Routes to Impedimetric Immunosensors, DNA-Sensors, and Enzyme Biosensors. *Electroanalysis* **2003**, *15*, 913−947.
(31) Revenga-Parra, M.; Garcia, T.; Pariente, F.; Lorenzo, E.; Alonso, C. Effects of Ionic Strength and Probe DNA Length on the Electrochemical Impedance Spectroscopic Response of Biosensors. *Electroanalysis* **2011**, *23*, 100−107.
(32) Baur, J.; Gondran, C.; Holzinger, M.; Defrancq, E.; Perrot, H.; Cosnier, S. Label-Free Femtomolar Detection of Target DNA by Impedimetric DNA Sensor Based on Poly (pyrrole-nitrilotriacetic acid) Film. *Anal. Chem.* **2010**, *82*, 1066−1072.
(33) Cai, W.; Peck, J. R.; Van Der Weide, D. W.; Hamers, R. J. Direct Electrical Detection of Hybridization at DNA-Modified Silicon Surfaces. *Biosens. Bioelectron.* **2004**, *19*, 1013−1019.
(34) Xu, D. K.; Xu, D. W.; Yu, X. B.; Liu, Z. H.; He, W.; Ma, Z. Q. Label-Free Electrochemical Detection for Aptamer-Based Array Electrodes. *Anal. Chem.* **2005**, *77*, 5107−5113.
(35) Gooding, J. J. Electrochemical DNA Hybridization Biosensors. *Electroanalysis* **2002**, *14*, 1149−1156.
(36) Wang, Y.; Li, C. J.; Li, X. H.; Li, Y. F.; Kraatz, H. B. Unlabeled Hairpin-DNA Probe for the Detection of Single-Nucleotide Mismatches by Electrochemical Impedance Spectroscopy. *Anal. Chem.* **2008**, *80*, 2255−2260.
(37) Chang, H. X.; Li, J. H. Electrochemical Impedance Probing of Transcriptional TATA Binding Protein Based on TATA Box Site-Specific *Binding. Electrochem. Commun.* **2009**, *11*, 2101−2104.
(38) Bogomolova, A.; Komarova, E.; Reber, K.; Gerasimov, T.; Yavuz, O.; Bhatt, S.; Aldissi, M. Challenges of Electrochemical Impedance Spectroscopy in Protein Biosensing. *Anal. Chem.* **2009**, *81*, 3944−3949.
(39) Diniz, F. B.; Ueta, R. R.; Pedrosa, A. M. D.; Areias, M. D.; Pereira, V. R. A.; Silva, E. D.; Da Silva, J. G.; Ferreira, A. G. P.; Gomes, Y. M. Impedimetric Evaluation for Diagnosis of Chagas' Disease: Antigen−

DOI: 10.1021/acsami.7b15014
ACS Appl. Mater. Interfaces 2017, 9, 44231−44240

Antibody Interactions on Metallic Eletrodes. *Biosens. Bioelectron.* **2003**, *19*, 79−84.
(40) Radi, A.; Sánchez, J. L. A.; Baldrich, E.; O'Sullivan, C. K. Reagentless, Reusable, Ultrasensitive Electrochemical Molecular Beacon Aptasensor. *J. Am. Chem. Soc.* **2006**, *128*, 117−124.
(41) Figueroa, A. A.; Cattie, D.; Delaney, S. Structure of Even/Odd Trinucleotide Repeat Sequences Modulates Persistence of Non-B Conformations and Conversion to Duplex. *Biochemistry* **2011**, *50*, 4441−4450.

DOI: 10.1021/acsami.7b15014
ACS Appl. Mater. Interfaces 2017, 9, 44231−44240